

Layered ferromagnet-superconductor structures: the state and proximity effects

Klaus Halternan

Sensor and Signal Sciences Division, Naval Air Warfare Center, China Lake, California 93355

Oriol T. Valls^{*}

School of Physics and Astronomy and Minnesota Supercomputer Institute, Minneapolis, Minnesota 55455

(Dated: March 22, 2024)

We investigate clean multilayered structures of the SFS and SFSFS type, (where the S layer is intrinsically superconducting and the F layer is ferromagnetic) through numerical solution of the self-consistent Bogoliubov-de Gennes equations for these systems. We obtain results for the pair amplitude, the local density of states, and the local magnetic moment. We find that as a function of the thickness d_F of the magnetic layers separating adjacent superconductors, the ground state energy varies periodically between two stable states. The first state is an ordinary "0-state", in which the order parameter has a phase difference of zero between consecutive S layers, and the second is a " π -state", where the sign alternates, corresponding to a phase difference of π between adjacent S layers. This behavior can be understood from simple arguments. The density of states and the local magnetic moment reflect also this periodicity.

PACS numbers: 74.50+ r, 74.25.Fy, 74.80.Fp

I. INTRODUCTION

The study of layered ferromagnet-superconductor (F/S) heterostructure has sustained the active interest of many researchers. This is due in great part to continuing and recent progress in the preparation and fabrication of multilayer systems, and to the potential use of such heterostructures in various important applications. In particular, structures consisting of alternating ferromagnet (F) and superconductor (S) layers may exhibit, in certain cases, a ground state in which the difference between the order parameter phase of adjacent superconductor layers equals π . These are the so called " π junctions". These F/S hybrid structures offer advances in the field of nanoscale technology, including quantum computing,¹ where the implementation of a quantum two-level system is based on superconducting loops of π junctions. Furthermore, artificial composites involving a superconductor sandwiched between two ferromagnets, the design of which follows from giant magnetoresistive (GMR) devices, show potential use as spin-valves^{2,3} and nonvolatile memory elements.⁴ An essential principle behind many of these spin-based devices is the damped oscillatory nature of the Cooper pairs in the ferromagnet region, and the associated phase shift in the superconducting order parameter.

The coupling between nearby superconductors separated by a ferromagnet is a property that follows from the proximity effects, which in the context of F/S multilayers consist of the existence of superconducting correlations in the ferromagnet and magnetic correlations in the superconductor, arising from their mutual influence. The resulting superconducting phase coherence is quantified by the pair amplitude $F(r) = \langle \hat{h}_\#(r) \hat{h}_\#^\dagger(r) \rangle$, where the $\hat{h}_\#$ are the usual annihilation operators. It is now well established that the leakage of superconductivity is due to the process of Andreev reflection⁵, whereby a quasi-

particle incident on a F/S interface is retroreflected as a quasihole of opposite spin. It is in turn the coherent superposition of these states, spin split by the exchange field in the ferromagnet, that ultimately leads to damped oscillations of $F(r)$ in the magnet, with a characteristic length ξ_F typically much smaller than the superconducting coherence length ξ_0 . These oscillations are akin to high field oscillatory phenomena described a long time ago.^{6,7} In the absence of currents and magnetic fields, the modulation of the order parameter determines whether two neighboring superconductor layers share a stable or 0 phase difference. For a multilayer F/S heterostructure with ferromagnet layers of order ξ_F in width, it is intuitively evident, taking into account the continuity of $F(r)$ across the F/S interface and the particular oscillatory nature of the pair amplitude in the ferromagnet, that a configuration will result in which it is energetically favorable to have a phase difference of π , rather than zero, between successive superconducting layers. This indeed turns out to be the case.

Although recently there has been a surge of interest in the study of F/S multilayer structures, (see e.g. the theoretical work of Refs. 8,9,10,11,12,13,14,15,16, 17,18,19,20,21,22,23,24,25 and the experimental work discussed below) work on superconductor-ferromagnet-superconductor (SFS) Josephson junctions started long ago.²⁶ The Josephson current was calculated for a short weak link in the clean limit, and found to exhibit oscillations as a function of the ferromagnet exchange field.²⁷ It was later demonstrated that for an SFS sandwich obeying the dirty limit conditions, the critical current oscillates as a function of the thickness of the magnet, and of the exchange field.¹⁴ A more detailed analysis of dirty π junctions near the critical temperature allowed for differing transparencies of the ferromagnet-superconductor interfaces.¹⁵ Many interesting phenomena have been proposed or discussed. Calculations were

more recently performed for an SFS junction with arbitrary impurity concentration. For non-homogeneous magnetization,^{17,25} the superconductor may exhibit a nonzero triplet component extending well into the magnet. For quasi two-dimensional, tight-binding, F/S atomic-scale multilayers, the ground state was shown in some cases to be the $\uparrow\downarrow$ state¹⁸, and the density of states (DOS) exhibited prominent features that depend critically on the exchange field and transfer integrals.¹⁹ For multilayer structures consisting of two ferromagnets and an insulator sandwiched between two superconductors, an enhancement of the Josephson current was predicted^{20,21} for antiparallel alignment of the magnetization in the ferromagnet layers. Spin-orbit scattering^{16,22} and changing the relative orientation angle of the in-plane magnetizations²³ were shown to significantly modify the behavior of the dc Josephson current.

The rapidly evolving theoretical views compounded with technological advancements which permit the fabrication of well-characterized heterostructures, has prompted a considerable number of experimental investigations of coupling on several fronts. A study of the superconducting transition temperature for F/S multilayers revealed oscillatory behavior as a function of ferromagnet thickness.²⁸ For junctions involving relatively weak ferromagnets, variations in temperature can induce a crossover from $\uparrow\downarrow = 0$ to the $\uparrow\uparrow$ state, and this was observed²⁹ as oscillations of the critical current versus temperature. The transition to the $\uparrow\uparrow$ state is also reflected in critical current measurements for Josephson junctions in which the ferromagnet layer separating the two superconductors was systematically varied.³⁰ The superconducting phase was measured directly³¹ using SQUID's made of junctions, demonstrating a half-quantum flux shift in the diffraction pattern. Direct evidence of the oscillatory behavior of the superconducting correlations in the ferromagnet was found through tunneling spectroscopy measurements which yielded inversions in DOS for a thin ferromagnetic film, in contrast with the behavior in a superconductor.³²

A common feature that pervades most of the theoretical work mentioned above is the use of quasiclassical formalisms, often compounded by the neglect of self-consistency for the space dependent pair potential, $\langle r \rangle$. These approximations do have the advantage of providing an accessible and efficient method to approximately calculate properties of inhomogeneous superconducting systems, while avoiding the cumbersome numerical issues that arise when attempting to solve the corresponding, much more complicated, self-consistent microscopic equations. The general underlying drawback of such approximations however, is the elimination from consideration of phenomena at the atomic length scale given by the Fermi wavelength, λ_F , as can be seen in the derivation of the Eilenberger equations.³³ Further approximations follow when the assumption is made that the mean free path is much shorter than λ_0 , in which case the Eilenberger equations reduce to the widely used Us-

adel equations.³⁴ The elimination of the relatively small length scales poses problems for quasiclassical methods (even when self-consistent) when interfacial scattering is involved,¹⁶ or when the geometry or potentials have sharp variations on the atomic scale. These issues, of increasing experimental importance given the ever improving quality of the experimental samples, often require nontrivial effective boundary conditions that must supplement the basic equations. The problem worsens when dealing with multilayer structures, where the successive reflections and transmission of quasiparticles creates closed trajectories³⁵ that may render the quasiclassical approximation scheme inapplicable.

In this paper we investigate the proximity effect and associated electronic properties of clean three-dimensional F/S multilayer structures comprised of alternating superconductor and ferromagnet layers. Our emphasis is on the study of the existence of pair potential behavior of the $\uparrow\downarrow$ type. We implement a complete self-consistent microscopic theory that treats all the characteristic length scales on an equal footing, and thus can accommodate all quantum interference effects that are likely to be pertinent. The problem will be solved from a wave function approach using the Bogoliubov-de Gennes (BdG) equations. To do so, we extend an earlier method³⁶ used for a single F/S structure, to allow for a more complicated geometry, consisting of an arbitrary number of layers. Self-consistency is rigorously included, as it has been demonstrated^{36,37} that this is essential in the study of the proximity effect at F/S interfaces.

We present in Sec.II the geometry and the numerical approach we take to solve the microscopic BdG equations and obtain the self-consistent energy spectra (eigenvalues and eigenfunctions). We also explain in some detail how the local DOS and the ground state energy are calculated. In Sec.III we first present our results for SFS structures and show examples of the relevant quantities: these include first of all the pair amplitude, which is used to illustrate the cases in which either the 0 or $\uparrow\downarrow$ state is energetically favored. The thickness of the F layer or layers turns out to be the decisive parameter, with the zero and $\uparrow\downarrow$ states periodically alternating in stability as this quantity varies. The experimentally accessible DOS averaged over a superconducting layer is next discussed: results for both the sum and the difference of the up and down spin terms are presented and their correlation with the zero or $\uparrow\downarrow$ states demonstrated. Results for the local magnetic moment, which we show how to calculate from the spin-dependent local DOS, are also given: in the superconductor this quantity measures the penetration of magnetic correlations. We analyze also, in a similar fashion, a more complicated $\uparrow\downarrow$ layer structure, discuss the similarities and differences between the two geometries, and the generalization of our results to more complicated structures. Finally in Sec.IV we briefly summarize our results and discuss potential experimental implications and future work.

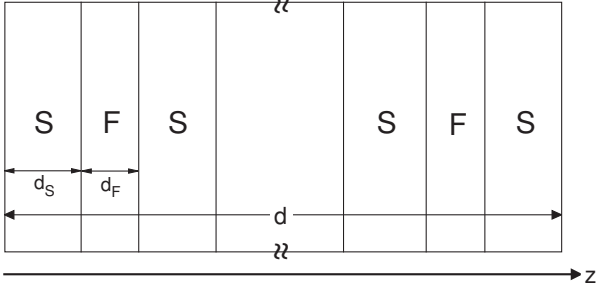


FIG. 1: Schematic of the model geometry used in this paper. The total thickness in the z direction is d , and the thicknesses of the S and F layers are d_S and d_F as indicated. There is a total number N_L of layers $N_L = 3$ and $N_L = 5$ in this work, with the outer ones being superconducting. The line breaks in the middle region denote repetition.

II. METHOD

In this paper we consider a semi-infinite multilayer structure of total length d in the z -direction, consisting of an odd number N_L of alternate superconductor (S) and ferromagnetic (F) layers, each of width d_S and d_F respectively (see Fig. 1). The sandwich configuration is such that the complete structure begins and ends with a superconductor layer. The free surfaces at $z = 0$ and $z = d$ are specularly reflecting. The basic methodology we use is an extension of that which has been previously discussed.^{36,37} Upon taking into account the translational invariance in the $x-y$ plane, one can immediately write down the BdG³⁸ equations for the spin-up and spin-down quasiparticle and quasihole wave functions ($u_n; v_n$),

$$\begin{pmatrix} H & h_0(z) \\ h_0(z) & [H + h_0(z)] \end{pmatrix} \begin{pmatrix} u_n(z) \\ v_n(z) \end{pmatrix} = \epsilon_n \begin{pmatrix} u_n(z) \\ v_n(z) \end{pmatrix} \quad (1)$$

where the free-particle Hamiltonian is defined as,

$$H = \frac{1}{2m} \frac{\partial^2}{\partial z^2} + \epsilon_{\perp} \quad E_F(z); \quad (2)$$

Here ϵ_{\perp} is the transverse kinetic energy, the ϵ_n are the quasiparticle energy eigenvalues, and $h_0(z)$ is the pair potential, described below. The magnetic exchange energy

$h_0(z)$ is equal to a constant h_0 in the ferromagnetic layers, and zero elsewhere. A potential $U(z)$ describing interface scattering can easily be added to Eqn. 2. We define the quantity $E_F(z)$ to equal E_{FM} in the magnetic layers, so that in these regions, $E_F^+ = E_{FM} + h_0$, and $E_F^- = E_{FM} - h_0$. Likewise, in the superconducting layers, $E_F(z) = E_{FS}$. The dimensionless parameter $I = h_0/E_{FM}$ characterizes the strength of the magnet. At $I = 1$, one therefore reaches the half-metallic limit. From the symmetry of the problem, the solutions for the other set of wavefunctions ($u_n^{\#}; v_n^{\#}$) are easily obtained from those of Eqns. (1) by allowing for both positive and negative energies. The BdG equations are completed by the self-consistency condition for the pair potential,

$$h_0(z) = \frac{g(z)}{2} \sum_n \left[u_n^{\#}(z) v_n^{\#}(z) + u_n(z) v_n(z) \tanh\left(\frac{\epsilon_n}{2T}\right) \right]; \quad (3)$$

where T is the temperature, $g(z)$ is the effective coupling describing the electron-electron interaction, which we take to be a constant g within the superconductor layers and zero within the ferromagnetic layers, and ϵ_D is the Debye energy. We have not included spin-orbit coupling, and assumed that all of the F layers are magnetically aligned and hence²⁵ considered singlet pairing only, in the s -wave.

We solve³⁷ Eq. (1) by expanding the quasiparticle amplitudes in terms of a finite subset of a set of orthonormal basis vectors, $u_n(z) = \sum_q u_{nq} u_q(z)$, and $v_n(z) = \sum_q v_{nq} v_q(z)$. We use the complete set of eigenfunctions $u_q(z) = \frac{1}{\sqrt{2d}} \sin(k_q z)$, where $k_q = \frac{q\pi}{d}$, and q is a positive integer. The finite range of the pairing interaction ϵ_D permits the number N of such basis vectors to be cut off in the usual way.³⁶ Once this is done, we arrive at the following $2N \times 2N$ matrix eigensystem,

$$\begin{pmatrix} H^+ & D \\ D & H^- \end{pmatrix} \begin{pmatrix} u_n \\ v_n \end{pmatrix} = \epsilon_n \begin{pmatrix} u_n \\ v_n \end{pmatrix}; \quad (4)$$

where $T_n = (u_{n1}^{\#}; \dots; u_{nN}^{\#}; v_{n1}^{\#}; \dots; v_{nN}^{\#})$: The matrix elements $H_{qq^0}^{\pm}$ connecting q to q^0 are constructed from the real-space quantities in Eq.(1),

$$\begin{aligned} H_{qq^0}^+ &= \int_0^d dz \frac{1}{2m} \frac{\partial^2}{\partial z^2} u_q(z) \frac{\partial^2}{\partial z^2} u_{q^0}(z) + \epsilon_{\perp} \int_0^d dz u_q(z) u_{q^0}(z) \\ &= \frac{k_q^2}{2m} \delta_{qq^0} + \epsilon_{\perp} \delta_{qq^0} \end{aligned} \quad (5a)$$

The expression for $H_{qq^0}^-$ is calculated similarly. The off-diagonal matrix elements D_{qq^0} are given as,

$$D_{qq^0} = \int_0^d dz u_q(z) h_0(z) u_{q^0}(z); \quad (5b)$$

After performing the integrations, Eq.(5a) can be expressed as

$$H_{qq^0}^+ = \sum_{n=2}^{N_X-1} \frac{E_F}{d} \frac{\hbar \sin[(k_q - k_{q^0})(d_F + d_S) = 2\pi] \sin[(k_q - k_{q^0})(d_F + d_S) = 2\pi - \phi]}{(k_q - k_{q^0})} \\ + \frac{\sin[(k_q + k_{q^0})(d_F + d_S) = 2\pi - \phi]}{(k_q + k_{q^0})} \frac{\sin[(k_q + k_{q^0})(d_F + d_S) = 2\pi]}{(k_q + k_{q^0})} \\ + \frac{E_{FS}}{d} \frac{\hbar \sin[(k_q - k_{q^0})(d_F + d_S) = 2\pi - \phi]}{(k_q - k_{q^0})} \frac{\sin[(k_q - k_{q^0})(d_F + d_S) = 2\pi]}{(k_q - k_{q^0})} \\ + \frac{\sin[(k_q + k_{q^0})(d_F + d_S) = 2\pi]}{(k_q + k_{q^0})} \frac{\sin[(k_q + k_{q^0})(d_F + d_S) = 2\pi - \phi]}{(k_q + k_{q^0})} ; \quad q \neq q^0; \quad (6a)$$

where the sum is over even integers only. The diagonal matrix elements are somewhat simpler, and are written,

$$H_{qq}^+ = \frac{k_q^2}{2m} + \frac{E_F}{2d} N_L d_F \frac{1}{k_q} \sum_{n=2}^{N_X-1} \sin[nk_q(d_F + d_S) - \phi] \sin[nk_q(d_F + d_S)] \\ + \frac{E_{FS}}{2d} N_L d_S \frac{1}{k_q} \sum_{n=2}^{N_X-1} \sin[nk_q(d_F + d_S)] \sin[nk_q(d_F + d_S) - \phi] : \quad (6b)$$

The self-consistency condition, Eq.(3), is now transformed into,

$$(z) = \frac{(z)}{k_F d} \sum_{p \neq q} \sum_{q^0} \frac{\hbar}{d} u_{np}^* v_{np^0}^{\#} + u_{np}^{\#} v_{np^0}^* \sin(k_p z) \sin(k_{p^0} z) \tanh(\epsilon_n = 2T); \quad (7)$$

where $(z) = g(z)N(0)$, and $N(0)$ is the DOS for both spins of the superconductor in the normal state. The quantum numbers n encompass the continuous transverse energy ϵ_n , and the quantized longitudinal momentum index q .

The primary quantity of interest is the local density of one particle excitations in the system, $N(z; \epsilon)$. Current experimental tools such as the scanning tunneling microscope (STM) have atomic scale resolution, and make this quantity experimentally accessible. Since it is assumed that well defined quasiparticles exist, the tunneling current is simply expressed as a convolution of the one-particle spectral function of the STM tip with the spectral function for the ferromagnet-superconductor system.³⁹ The resultant tunneling conductance, which is proportional to the DOS, is then given as a sum of the individual contributions to the DOS from each spin channel. We have:

$$N(z; \epsilon) = N_{\#}(z; \epsilon) + N_{\#}(z; \epsilon); \quad (8)$$

where the local DOS for each spin state is given by

$$N_{\#}(z; \epsilon) = \sum_n \frac{\hbar}{d} [u_n^{\#}(z)]^2 f^0(\epsilon_n) + [v_n^{\#}(z)]^2 f^0(\epsilon_n + \epsilon_F); \quad (9a)$$

$$N_{\#}(z; \epsilon) = \sum_n \frac{\hbar}{d} [u_n^{\#}(z)]^2 f^0(\epsilon_n) + [v_n^{\#}(z)]^2 f^0(\epsilon_n + \epsilon_F); \quad (9b)$$

Here thermal broadening is accounted for in the term involving the derivative of the Fermi function f , $f^0(\epsilon) = -\partial f / \partial \epsilon$.

We shall see below that we will also need to compare different self-consistent states. In general this is done in terms of the free energy. However, we will consider here only the low temperature limit. For $T \rightarrow 0$, the entropy term can be neglected, as it vanishes proportionally to T^2 . In this case all we need is the ground state energy E_0 . In evaluating this quantity some care must be taken in properly including all energy shifts, even in the bulk case^{40,41}. In the inhomogeneous case the result⁴² can be written as:

$$E_0 = \int_0^d dz \int_1^{Z_0} N(z; \epsilon) d\epsilon + \frac{1}{g} \langle \sum_i \epsilon_i \rangle \quad (10)$$

where the angular brackets in $\langle \sum_i \epsilon_i \rangle$ denote the spatial average, and $N(z; \epsilon)$ is given in Eqn. 8. One can rewrite E_0 in a somewhat more standard way:

$$E_0 = \sum_{p,n} \frac{\hbar}{d} \frac{1}{2} (v_{np}^{\#})^2 + (v_{np}^{\#})^2 + \frac{1}{g} \langle \sum_i \epsilon_i \rangle; \quad (11)$$

which in principle gives E_0 in terms of the calculated excitation spectra.

III. RESULTS

In this section we present and discuss the results that we have obtained through our numerical solution of the matrix eigensystem Eq. (4) and the self-consistency condition Eq. (7). We will study the two cases of $N_L = 3$ and $N_L = 5$, that is, SFS and SFSFS structures separately. We consider only "regular" structures in which all S layers have the same thickness d_S , which we will take to be a fixed value larger than ξ_0 , while the F layers, when there is more than one, have all the same thickness, d_F , which we will vary. With the assumption that no current flows across the sample, the quantity $\psi(z)$ can be taken to be real, but it can in principle switch sign (zero or \pm state) in going from one S layer to the next.

In our calculations we have studied two different values of the parameter I , $I = 0.5$ and $I = 1$. We have set the superconducting correlation length ξ_0 to $\xi_0/k_F = 50$, where k_F is the Fermi wavevector of the superconductor, and taken $\hbar v_F = E_{FS} = 0.1$ for the dimensionless Debye energy cutoff. It follows from previous studies³⁷ that the first of these parameters simply sets the overall length scale in the superconductor and is of little relevance whenever d_S exceeds ξ_0 , as will be the case here, while the second is unimportant at low temperatures (the limit that we will consider), as it simply sets the scale for T_C . We have also assumed that there is no oxide barrier between the layers and that the "mismatch parameter" $\epsilon = (E_{FM} - E_{FS})$ is unity. A nonzero barrier height would in general diminish the amplitude of all the phenomena discussed here, without qualitatively altering the results. The possibility of varying ϵ is more complicated: this parameter³⁷ determines, together with I , the basic spatial periodicity of the problem, $\xi_F = (\epsilon^2 + k_F^2)^{-1/2}$, (where k_+ and k_- are respectively the Fermi wavevectors of the parabolic up and down spin bands in the ferromagnet) which we shall see is very important here. Furthermore, the amplitude of the oscillatory behavior found in simpler SF structures decreases³⁷ with ξ_F .

As explained in previous work (see Refs. 36,37), the self-consistent solution to these equations is obtained iteratively: one makes a suitable initial guess for $\psi(z)$, diagonalizes the system Eqn. (4) for that guess, and computes an iterated $\psi(z)$ from (7). The process is then repeated until convergence is obtained. The technicalities for the self-consistent solution of these equations were extensively discussed in previous work^{37,43}. The diagonalization in terms of the orthonormal basis chosen must be performed for each value of η in the appropriate range. We took here $N_\eta = 5000$ different values of η , except as indicated below, and the number of basis functions required for convergence was up to $N = 1000$. The self-consistent solution process is terminated when the relative error between consecutive iterated values of $\psi(z)$ nowhere exceeds 10^{-4} . We have found that the number of iterations needed to achieve self-consistency can be quite large: in most cases, it exceeds fifty.

Because our objective here is to discuss the possible states, in starting the iteration process we make two different initial guesses: one is of the ordinary "zero" state form, where the initial guess has the same sign (conventionally positive) in all the superconducting layers, and one of the \pm form, where it alternates sign from one S layer to the next. We have found that in some cases, for example for SFS structures with small d_S (i.e., $< \xi_0$), and $d_F < \xi_F$, the self-consistent $\psi(z)$ typically converges to either a 0 or \pm -state regardless of the initial guess, depending on d_F . A similar trend holds for the small d_S \pm -layer SFSFS system but over a broader d_F range. However, for the regular structures that we will focus on here, with $d_S > \xi_0$, two different self-consistent solutions are always obtained, one of the zero and one of the \pm type, according to the type of initial guess. We interpret this as showing that two local minima of the free energy exist. We then have to determine the stable minimum by calculating the free energy (or rather, at low temperature, the ground state energy) of both self-consistent states, as discussed below, and comparing them.

A. SFS

We consider first the case of an SFS sandwich. Preliminary investigations showed that the situation of interest occurs when the magnetic layer is not too thick. This is as expected, since the overall length over which the superconducting correlations penetrate (in an oscillatory way) into the magnet is characterized by $(k_+^2 + k_F^2)^{-1/2}$, which at the relatively large values of I considered here is fairly small. Thus, we have taken in the studies presented here a thickness $k_S d_S = 300$ for the superconducting layers, and the parameter $k_S d_F$ meanwhile, is varied in the range between one and twenty. The choice of $k_S d_S$ determines, through standard BCS theory relations, the value of the ratio of the superconductor Fermi energy to the bulk order parameter.

As explained above, results were obtained by iteration from two initial configurations of $\psi(z)$, with the initial guesses corresponding to opposite signs for the pair potential in each of the two S layers. For the range of parameters considered here, both initial guesses led in all cases to self-consistent configurations, which were either of the zero or of the \pm types, according to the initial guess. This is described in Fig. 2, where we show examples of the two self-consistent solutions for the pair amplitude $F(Z)$, as a function of the dimensionless distance $Z = k_S z$. It is not surprising that both types of solutions are found: it is after all obvious that in the limit where d_F is sufficiently large, both solutions must exist and be degenerate. The pair amplitude $F(z) = g(z)$ does not vanish identically in the magnetic region, but it exhibits the well-known oscillations. In the superconductor, it rises in absolute value towards the bulk result, away from the S/F interfaces. Results are shown for two values of I and two values of $k_S d_F$. We can see that in

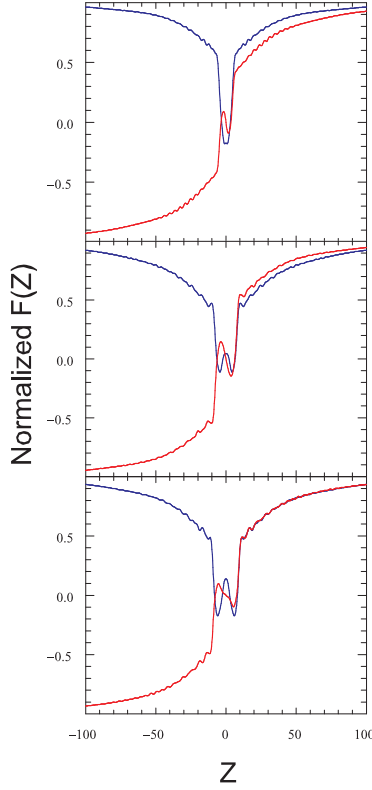


FIG. 2: (Color online). Results for the pair amplitude $F(Z)$, normalized to the bulk superconductor value, as a function of $Z = k_S z$, in an SFS structure. The dimensionless thickness of the S portions is $k_S d_S = 300$, while the corresponding values of the dimensionless thickness of the intervening F layer are (from top to bottom) $k_S d_F = 10; 16; 19$. The blue (solid) lines represent self-consistent solutions of the zero type, and the red lines alternative self-consistent solutions of the state type. The value of I is 0.5 and the superconducting correlation length is $\xi_0 = 50$.

certain cases, depending on the thickness of the F layer, $F(z)$ in the superconductor (and hence $F(Z)$) is larger, in absolute value, for the 'zero' than for the state (see top panel), while in some other cases (middle panel) the opposite occurs, and for yet some other d_F values (see the bottom panel) there is no observable difference. Intuitively, this happens because of the different way, depending on $k_S d_F$, in which the pair amplitude in the two superconductor regions must adjust itself to the oscillations in the magnet. That the oscillatory behavior of the pair amplitude in the F layer is clearly different for the zero and state solutions can be seen by careful examination of the portion of the plots which lies in the F region.

To find out the most stable configuration, one must compute the difference in the ground state energies, or equivalently the condensation energies, of the zero and state solutions. This can be done in principle by using Eqn. (11). In practice this is computationally very difficult: the value of E_0 for each state must be computed separately

from its own spectrum (which can consist of up to 10^6 eigenstates), and the results subtracted. Since each E_0 includes the normal state energy, which is many orders of magnitude larger than the condensation energy sought, this requires extreme numerical accuracy. The problem is exacerbated because the "logarithmic" last term in the right side of Eqn. (11) is in itself much larger than the condensation energy (and the latter is itself considerably larger, as we shall see below, than the condensation energy difference between the two states), and must be exactly canceled by a portion of the first term. This is a well-known problem even in the bulk case, where great care has to be taken⁴⁰ to make the delicate cancellation analytically explicit. We have found it technically impractical to numerically compute E_0 from Eqn. (11) for all cases considered⁴⁴ with the required precision. However, by using increased values of N_z and N in a few selected cases we have been able to verify that the ground state condensation energy (that is, after subtracting the normal ground state energy E_{0n} calculated for the same geometry and parameter values except for setting $g = 0$) for either the zero or state solutions is, for the cases considered here where d_F is small and $d_S \gg \xi_0$, approximately given by:

$$E_0 - E_{0n} \approx N(0) \hbar^2 j^2 i: \quad (12)$$

This result is, a posteriori not surprising at all in the limit of large d_S and small d_F , as it is quite similar to what is found⁴⁵ analytically for the bulk: in that case j^2 is exactly 0.5 and the spatial average is of course replaced by the uniform bulk value. In our case we find the coefficient $j^2 < 0.5$ within our numerical uncertainty. The right side of Eqn. (12) is of course very easy to compute. Thus, we have adopted a procedure based on Eqn. (12) to compare condensation energies for the two competing states.

The results are shown in Figure 3. The quantity plotted there is the difference between the values of $\hbar^2 j^2 i$ for the zero and state solutions normalized to $N(0) \hbar^2 j^2 i_0$, where i_0 is the bulk gap. This normalization corresponds to twice the bulk value limit of the condensation energy. This is then a dimensionless measure of the condensation (or equivalently, ground state) energy difference between the self-consistent zero and state configurations, (see Eqn. (12)). This normalized energy difference is plotted as a function of the dimensionless thickness $k_S d_F$ of the intermediate F layer, which is sandwiched between thick ($k_S d_S = 300$) S layers. We see that the difference in energies is, as one would expect, only a small fraction (about one tenth at the most) of the bulk condensation energy. We also see that it is an oscillatory function of $k_S d_F$. Comparison of the top and bottom panels (which correspond to $I = 0.5$ and $I = 1$ respectively) shows that the rough periodicity of these results is approximately given by $(k_F^* - k_F)^{-1}$, and it is in fact very similar³⁷ quantitatively to the oscillatory behavior of the pair amplitude $F(z)$ in a thick magnetic layer. At small $k_S d_F$, the zero state is obviously very favored, as one would expect, while in the limit of large $k_S d_F$ the energy difference is of course zero, reflecting

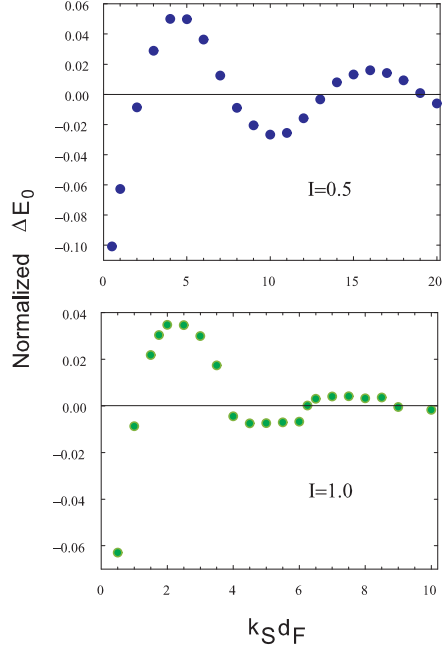


FIG. 3: (Color online). The difference in condensation energies, E_0 , between the zero and π states for an SFS sandwich in the low temperature limit, normalized to $N(0)_0^2$, calculated as explained in the text. The results are plotted as a function of the dimensionless thickness $k_S d_F$ of the ferromagnetic layer, for two values of I . At small d_F the zero state is favored. The periodicity of the results is determined by $(k_{\parallel} - k_{\#})^{-1}$, as expected.

the degeneracy of the two states. The influence of the parameter I is quite dramatic: in the half-metallic case (lower panel) the π state is more prominent and the zero state is generally speaking less favorable than for the intermediate value of I shown in the top panel.

We turn now to the density of states (DOS) for this geometry. Typical results are exhibited in Fig. 4, where we show the DOS, integrated over the superconducting region of thickness $k_S d_S = 300$, as a function of the energy normalized to Δ_0 . Results are shown for two values of I (top and bottom panels) and, for each value of I , at two values of $k_S d_F$, one corresponding to the case where the equilibrium state is of the zero type, and the other corresponding to the opposite situation. One can see that for $I = 0.5$ there are states in the gap, and that these states are more prominent in the π case where there is a zero energy small peak. At $I = 1$ the DOS results are also different: although for both of the cases shown there is a gap in the spectrum, the location of the peaks near

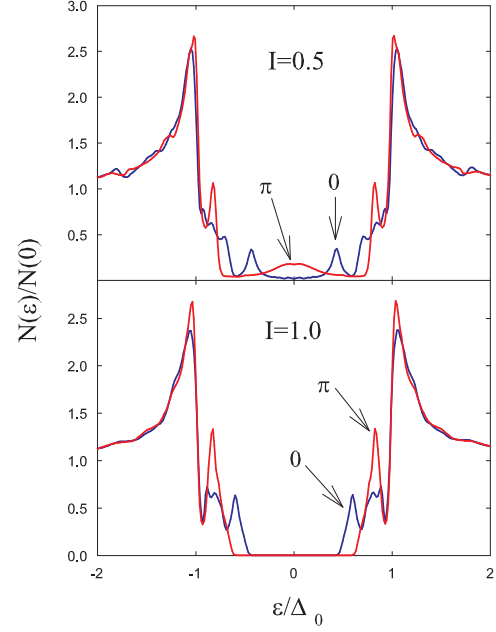


FIG. 4: (Color online). Density of states (DOS) results for SFS structures. The quantity plotted is the local DOS integrated over one S layer, normalized to $N(0)$. The energy is normalized to the bulk gap Δ_0 . The top panel shows results at $k_S d_F = 5$, where the stable state (see Fig. 3) is of the π type (red curve, labeled as π) and at $k_S d_F = 10$, where the zero state is more stable (blue solid curve, labeled 0). In the bottom panel, $I = 1$ and consistent with the doubling of I , the thicknesses displayed are halved to $k_S d_F = 2.5$ (π case) and $k_S d_F = 5$ (zero case). See text for discussion.

the gap edge is not the same for the zero and π states, with the π state peaks being more prominent and at higher energies in the latter case. Thus, there are genuine differences between the DOS of zero and π states, which may be experimentally observable.

It is also of interest to show the difference between the local DOS for up and down states, as defined by

$$N(z; \uparrow) - N(z; \downarrow) = N_{\#}(z; \uparrow): \quad (13)$$

This is done in Fig. 5, where results are shown for the two cases corresponding to those also displayed in the top panel of Fig. 4. The differential DOS shown is integrated over the thickness of one S layer, and normalized to the total normalized bulk DOS value. Because of the finite value of I , the results are not symmetric around zero energy. One can see that the energy structure at the gap edge is appreciably more prominent for the thickness value which corresponds to an equilibrium state, while for the zero state the structure is broader and more diffused.

An alternative way of illustrating the magnetic polarization effects, which has also the advantage of providing local information, is through the use of the local magnetic moment $m(z)$. This quantity is easily obtained by

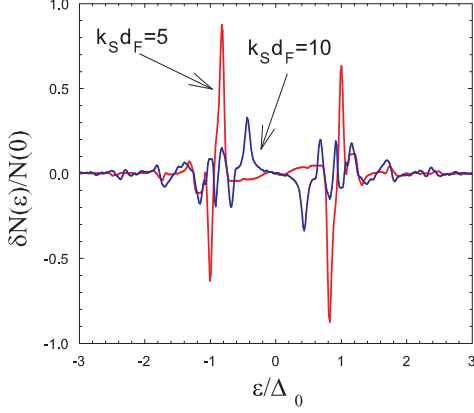


FIG. 5: (Color online). Differential density of states (DOS) between up and down spin states for SFS structures. The quantity plotted is that defined in Eq. (13), integrated over one S layer, and normalized to $N(0)$. Results are shown for $I = 0.5$ at $k_S d_F = 5$, where the stable state (see Fig. 3) is of the \uparrow type (red curve) and at $k_S d_F = 10$, where the zero state is more stable (blue solid curve).

integration of the local DOS results. One has:

$$m(z) = \frac{1}{B} \int_{-B}^B dz' N(z; z') f(z'); \quad (14)$$

where B is the Bohr magneton and the integral extends over the occupied states in the band. This can be cast in a more convenient form as:

$$m(z) = \frac{1}{B} [\langle n_{\uparrow}(z) \rangle - \langle n_{\downarrow}(z) \rangle]; \quad (15)$$

where $\langle n_{\sigma}(z) \rangle$ is the average number density for each spin subband, and is written in terms of the quasiparticle amplitudes as,

$$\langle n_{\sigma}(z) \rangle = \sum_n \int_{-B}^B dz' [u_n(z)]^2 f(\epsilon_n) + [v_n(z)]^2 [1 - f(\epsilon_n)]; \quad (16)$$

It is more instructive to plot $m(z)$ normalized to the corresponding integral of $N_{\uparrow}(z; z') + N_{\downarrow}(z; z')$. We denote this normalized quantity by $M(z)$ and we plot it, in units of the Bohr magneton, in Fig. 6. The two panels there correspond to values of I and $k_S d_F$ as in the corresponding top and bottom panels of Fig. 4. We see in this figure that for relatively small $k_S d_F$, the quantity plotted rises up sharply from the F/S interface and then has a slow modulation as it approaches its bulk value in the F layer. The magnetization does not vanish identically inside the superconductor: its behavior there consists of strongly damped oscillations, with an overall characteristic spatial decay on the order of a few Fermi wavelengths. The effect does not seem to depend strongly on whether one is dealing with zero or \pm states.

The self-consistent results displayed can also be interpreted as representing an effective, local value of $I(z)$,

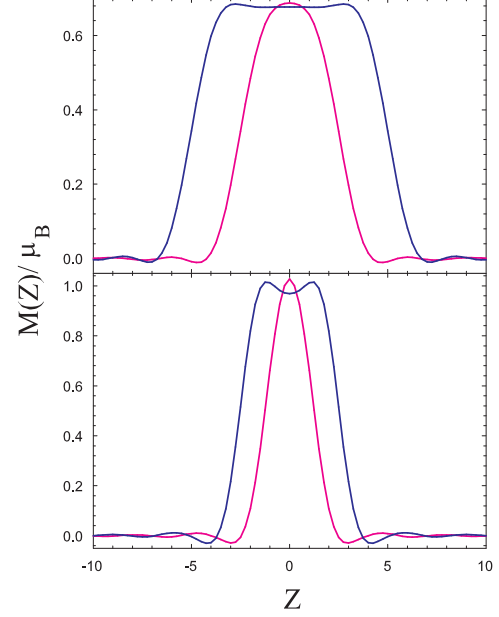


FIG. 6: (Color online). Normalized local magnetic moment as defined in the text and Eqn. 15. Results in the top and bottom panels correspond to the same values of I and thickness as in the corresponding panels of Fig. 4. Thus the top panel is for $I = 0.5$ and $k_S d_F = 5;10$, while the bottom panel is for $I = 1$ and $k_S d_F = 2.5;5$.

through the relation $M(z) = \frac{1}{B} [(1 + I(z))^{3/2} - (1 - I(z))^{3/2}] = [(1 + I(z))^{3/2} + (1 - I(z))^{3/2}]$. The quantity $I(z)$ is then the magnetic counterpart of the self-consistent $F(z)$, measuring directly the magnetic part of the proximity effect, that is, the leakage of magnetic correlations into the superconductor.

$$I(z) = \frac{1}{B} \int_{-B}^B dz' F(z; z') \quad (17)$$

In this subsection we consider the case of more complicated, n -layer structures. These are realizable experimentally²⁸ and therefore of considerable interest. As in the three layer case, we will study the situation where the three superconducting layers are relatively thick, taking again $k_S d_S = 300$ and the F layers are thin enough so that F/S proximity effects cannot be neglected.

We begin by considering (see Fig. 7) the pair amplitude $F(z)$. This figure is in every way analogous to Fig. 2, except for the insets, where we display in more detail the behavior of $F(z)$ in one of the ferromagnetic layers. Results for solutions of both the zero and the \pm type are shown. Both are obtained self-consistently, the first by starting from an initial guess in which the sign of the order parameter in the three S layers is always the same, and the second by starting with a guess in which the order parameter in the middle S layer is the opposite to

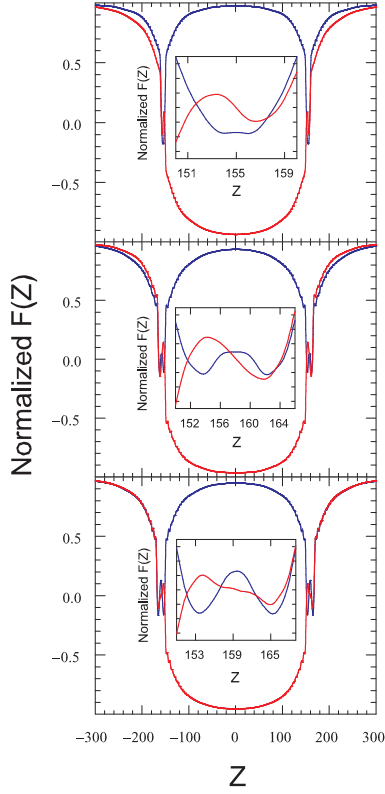


FIG. 7: (Color online). Results for the pair amplitude $F(Z)$, normalized to the bulk superconductor value, as a function of $Z = k_S z$, in an SFSFS structure, for $I = 0.5$. The dimensionless thickness of the S portions is $k_S d_S = 300$, and the corresponding values of the dimensionless thickness of the intervening F layer are (from top to bottom) $k_S d_F = 10; 16; 19$. The blue (solid) lines represent self-consistent solutions of the zero type, and the red lines of the π type. The insets are a magnification of one of the F regions. The vertical axis in the insets varies between ± 35 in dimensionless units.

that in the other two layers. Self-consistent solutions are always reached by iteration, for large d_S and d_F in the ranges shown, in either case. We observe the expected depletion of $F(z)$ near the F/S interfaces, and the subsequent approach towards its bulk value over the length scale ξ_0 , with the maximum $|F(z)|$ in the central S layer slightly reduced from the bulk ξ_0 . We also see in the main panels that depending on the value of $k_S d_F$, the absolute value of $F(z)$ in the superconductors varies periodically between being larger in the zero state to being larger in the π state, as was the case for three layer structures. The insets illustrate more clearly how the existence of the two states relates to the oscillations of $F(z)$ in the ferromagnetic region, which are very different in each case.

As in the three layer case, therefore, we find that there are two local minima of the free energy, corresponding to the zero and π alternatives. Again, the absolute minimum, at low temperature, must be found by comparing

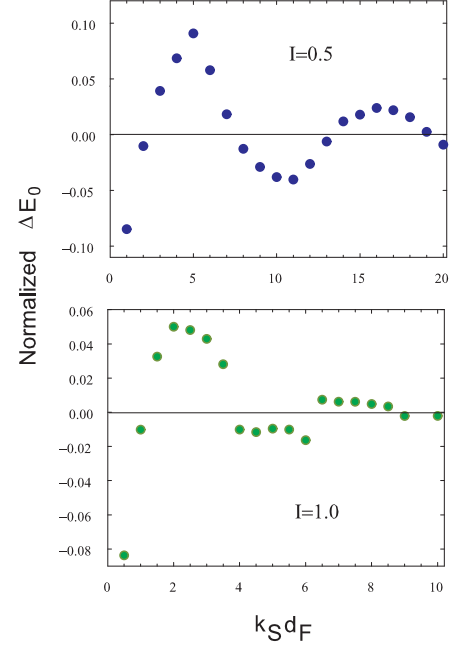


FIG. 8: (Color online). Difference in condensation energies, ΔE_0 , between the zero and π states for a five layer SFSFS system, calculated as explained in the text, and normalized to $N(0) \xi_0^2$, as in Fig. 3. This quantity is plotted as a function of the thickness $k_S d_F$ of each ferromagnetic layer. Results for two values of I are shown.

the two condensation energies. This we do in the same way as for the three layer case (see Eqn. 12 and associated discussion). The results are shown in Fig. 8, which should be compared with Fig. 3. The two figures are remarkably similar. In both cases the behavior is oscillatory, with the same approximate spatial periodicity related to that of the pair amplitude oscillations. Again, the obvious results that the zero state is favored at small $k_S d_F$ and that the two states are degenerate for large $k_S d_F$ are recovered. The three and five layer plots are not identical, however: in the latter case we find that the overall scale of the phenomenon is nearly a factor of two higher, as one can see by comparing the vertical axes. The first peak favoring the π state is higher and sharper for five layers. Although the effect of increasing the layer number is not as dramatic as that of increasing I , one can nevertheless assert from the trend that the oscillatory behavior with d_F would not only persist but would be even more prominent if the number of layers were further increased, as in superlattices.

A few selected DOS results for this SFSFS geometry are shown in Fig. 9, which should be viewed in comparison

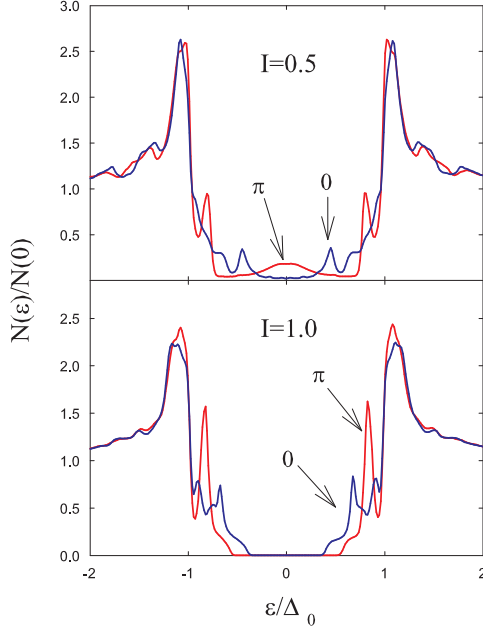


FIG. 9: (Color online). Density of states (DOS) results for SF/SFS structures. The local DOS integrated over one of the external S layers, normalized to $N(0)$, is plotted vs. the energy normalized to the bulk gap Δ_0 . The top panel shows results at $k_S d_F = 5$, where the stable state (see Fig. 8) is of the π type (red curve, labeled as π) and at $k_S d_F = 10$, where the zero state is more stable (blue solid curve, labeled 0). In the bottom panel, $I = 1$ and the thicknesses are $k_S d_F = 2.5$ (π case) and $k_S d_F = 5$ (zero case).

son with the analogous Fig. 4 for the SFS structure. The quantity plotted is averaged over one of the two outside S layers, and all parameters are chosen to be the same as in Fig. 4. The similarity between the two figures is at first sight very remarkable, although a second look shows that the structure of the subgap peaks is far from being the same, particularly for the zero state case, where additional shoulders appear at $I = 1$. One concludes again that many features, including the zero energy peak in the stable state of the top panel, are robust with respect to increasing the number of layers, and very likely to persist, and even become more obvious, in larger regular structures.

The differential DOS between up and down states for this geometry exhibits a behavior sufficiently similar to that displayed in Fig. 5 for the SFS case that there is no need to display it in a separate figure here. On the other hand, it is worthwhile to illustrate an example of the normalized local magnetic moment $M(z)$. This is done on Fig. 10, where this quantity, as defined in Eqn. 14 is plotted with the same normalization and parameter values as in the top panel of Fig. 6. The behavior for the two geometries is certainly similar, but one again sees that the magnetic penetration effects become more prominent as the number of layers increases from three to five. This is another indication that such effects are

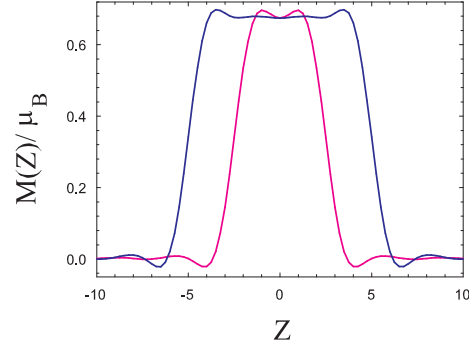


FIG. 10: (Color online). Normalized local magnetic moment for an SF/SFS structure, as defined in the text and Eqn. 14. Results are for $I = 0.5$ and $k_S d_F = 5, 10$.

very likely to be easier to observe in structures involving a larger number of layers.

IV. CONCLUSIONS

We have rigorously investigated the proximity effects that occur in clean multilayered F/S structures of the SFS and SF/SFS type. We used a microscopic wavefunction approach that does not coarse grain over length scales of order ξ_F , and thus accounts for atomic-scale effects. The space dependence of the pair amplitude $F(z)$ was obtained self-consistently by using an efficient numerical algorithm. From the calculated eigenstates, we were then able to obtain the experimentally relevant local magnetic moment, and the local density of states.

We have demonstrated that for all the cases considered, where the thickness d_S of the superconducting layers is much greater than ξ_0 and that of the ferromagnetic regions is relatively small, two local minima of the ground state energy exist, thus yielding self-consistent states of the 0 and π types. Through a careful analysis of the pair amplitude and excitation spectrum, we have calculated which of these two states is the actual ground state, with the lowest energy. The results show that the difference in condensation energies between the 0 and π states exhibits damped oscillations as a function of ferromagnet width, with the characteristic exchange-field dependent spatial period being given approximately as $2(\kappa_\pi - \kappa_F)^{-1}$, the same quantity which characterizes the oscillations of $F(z)$ in bilayers. The local DOS exhibits strikingly different behavior for two exchange fields that differed by a factor of two. For $I = 0.5$, the subgap DOS shows a gapless structure, with features that depend strongly on whether the ferromagnet width corresponds to the 0 or π state. The half-metallic case ($I = 1.0$) is on the other hand gapless in the range of d_F considered, and the modified

excitation spectrum reveals itself through the differing peaks in the DOS. To illustrate the leakage of magnetism into the superconductor, the differential DOS between the spin up and spin down states was presented for a SFS junction. The most prominent spin-splitting was seen for the σ -junction at energies $\epsilon = 0$. We believe that this represents an experimentally important signature for the σ state. We have also calculated the local magnetic moment for both the three and five layer cases, to give further insight into magnetic polarization effects. Although we found the results to be relatively insensitive to a 0 or σ state configuration, we were able to extract an effective local value of $I(z)$ in both the F and S layers.

The calculations and method used in this paper, although sufficiently general to include in the future more complicated effects (e.g. finite temperature, other pairing states, spin- $\uparrow\downarrow$ scattering, and impurities), were taken within the ballistic limit. This limit is appropriate for ferromagnetic layers whose width is less than the mean free

path, and this is consistent with our calculations, where we have taken $k_F d_F \approx 20$. The inclusion of interfacial scattering would likely have the effect of diminishing the proximity effect, without qualitatively altering the characteristic results. For bulk impurity scattering, the effective τ_F would involve not just I but also the diffusion length. It is the goal of future work to address these topics, and also others, including heterostructures comprised of a single superconductor sandwiched between two ferromagnets with arbitrary relative magnetization, F/S multilayers with a greater number of layers, and smaller superconductor widths, where geometrical and atomic-scale effects are likely to be more prevalent.

Acknowledgments

We thank Igor Zutic for many useful discussions.

Electronic address: klaus.haltemann@navy.mil

^y Electronic address: otvalls@um.nyu.edu

¹ G. B. Lattar, V. B. Geshkenbein, and L. B. Ioannidis, Phys. Rev. B 63, 174511 (2001).

² L. R. Tagirov, Phys. Rev. Lett. 83, 2058 (1999).

³ B. N. Adgomy and I. I. Mazin, Appl. Phys. Lett. 80, 3973 (2002).

⁴ S. Oh, D. Youm, and M. R. Beasley, Appl. Phys. Lett. 71, 2376 (1997).

⁵ A. F. Andreev, Zh. Eksp. Teor. Fiz. 46, 1823 (1964) [Sov. Phys. JETP 19, 1228 (1964)].

⁶ P. Fulde and A. Ferrell, Phys. Rev. 135, A550 (1964).

⁷ A. Larkin and Y. Ovchinnikov, Sov. Phys. JETP 20, 762 (1965).

⁸ N. M. Chitchev, W. Belzig, Y. V. Nazarov, and C. Bruder, JETP Letters 74, 96 (2001) [Pis'ma v ZhETF 74, 101 (2001)].

⁹ A. Y. Zyuzin, B. Spivak, M. Hruska, Euro. Phys. Lett. 62, 97 (2003).

¹⁰ A. Zenchuk and E. Goldobin, nlin.ps/0304053 (unpublished).

¹¹ A. F. Volkov, F. S. Bergeret, and K. B. Efetov, Phys. Rev. Lett. 90, 117006 (2003).

¹² M. Krawiec, B. L. Gyor'y, and J. F. Annett, Phys. Rev. B 66, 172505 (2002).

¹³ Z. Radovic, L. D. G. Ru'ic, and B. Vujcic, Phys. Rev. B 63, 214512 (2001).

¹⁴ A. I. Buzdin and M. Y. Kuprianov, Pis'ma Zh. Eksp. Teor. Fiz. 53, 308 (1991) [JETP Lett. 53, 321 (1991)].

¹⁵ A. Buzdin and I. Baladie, Phys. Rev. B 67, 184519 (2003).

¹⁶ E. A. Demler, G. B. A. Mol, and M. R. Beasley, Phys. Rev. B 55, 15174 (1997).

¹⁷ F. S. Bergeret, A. F. Volkov, and K. B. Efetov, Phys. Rev. B 64, 134506 (2001).

¹⁸ A. V. Andreev, A. I. Buzdin, and R. M. Osgood III, Phys. Rev. B 43, 10124 (1991).

¹⁹ V. P. Rokic, A. I. Buzdin, and L. D. G. Ru'ic, Phys. Rev. B 59, 587 (1999).

²⁰ F. S. Bergeret, A. F. Volkov, and K. B. Efetov, Phys. Rev.

Lett. 86, 3140 (2001).

²¹ V. N. Krivoruchko and E. A. Koshina, Phys. Rev. B 64, 172511 (2001).

²² V. N. Krivoruchko and R. V. Petryuk, Phys. Rev. B 66, 134520 (2002).

²³ Y. S. Barash, I. V. Bobkova, and T. Kopp, Phys. Rev. B 66, 140503(R) (2002).

²⁴ Z. Radovic, N. Lazarides, and N. Flytzanis, cond-mat/0305437 (unpublished).

²⁵ F. S. Bergeret, A. F. Volkov and K. B. Efetov, Phys. Rev. Lett. 90, 117006 (2003).

²⁶ For an early discussion of F/S effects, see the article by G. Deutscher and P. G. de Gennes in p. 1005 of Superconductivity, ed. by R. D. Parks, (Dekker, N.Y. 1969).

²⁷ A. I. Buzdin, I. N. Bulaeviskii, and S. V. Panyukov, Pis'ma Zh. Eksp. Teor. Fiz. 35, 147 (1982) [JETP Lett. 35, 178 (1982)].

²⁸ J. S. Jiang, D. Davidovic, D. H. Reich, and C. L. Chien, Phys. Rev. Lett. 74, 314 (1995).

²⁹ V. V. Ryzanov, V. A. Oboznov, A. Y. Rusanov, A. V. Veretennikov, A. A. Golubov, and J. Aarts, Phys. Rev. Lett. 86, 2427 (2001).

³⁰ T. Kontos, M. Aprili, J. Lesueur, F. Genet, B. Stephanidis, and R. Boursier, Phys. Rev. Lett. 89, 137007 (2002).

³¹ W. Guichard, M. Aprili, O. Bourgeois, T. Kontos, J. Lesueur, and P. Gandit, Phys. Rev. Lett. 90, 167001 (2003).

³² T. Kontos, M. Aprili, J. Lesueur, and X. G. Rison, Phys. Rev. Lett. 86, 304 (2001).

³³ G. Eilenberger, Z. Phys. 214, 195 (1968).

³⁴ K. D. Usadel, Phys. Rev. Lett. 25, 507 (1970).

³⁵ M. Ozana and A. Shelankov, J. Low Temp. Phys. 124, 223 (2001); M. Ozana, A. Shelankov, and J. Tobiska, cond-mat/0201199 (unpublished).

³⁶ K. Haltemann and O. T. Valls, Phys. Rev. B 65, 014509 (2002).

³⁷ K. Haltemann and O. T. Valls, Phys. Rev. B 66, 224516 (2002).

³⁸ P. G. de Gennes, Superconductivity of Metals and Alloys

- (Addison-Wesley, Reading, MA, 1989).
- ³⁹ See, e.g., F. Gygi and M. Schlüter, Phys. Rev. B 41, 822 (1990).
- ⁴⁰ M. Tinkham, Introduction to Superconductivity, (Krieger, Malabar FL) (1975).
- ⁴¹ A. L. Fetter and J. D. Walecka, Quantum Theory of many-particle systems, (McGraw-Hill, New York NY) (1971).
- ⁴² I. Kosztin, S. Kos, M. Stone, and A. J. Leggett, Phys. Rev. B 58, 9365 (1998).
- ⁴³ K. Halteman, PhD dissertation, University of Minnesota, 2002.
- ⁴⁴ Alternative numerical methods e.g. using infinite Fredholm determinants have been proposed (see Ref. 42 for a survey), but the precision problems remain.
- ⁴⁵ See among many others Ref. 40 page 29.